Preprint submitted to Engineering Structures
Published on Issue 171 (2018) pp 298-308
https://doi.org/10.1016/j.engstruct.2018.05.075

An effective computational design strategy for H_∞ vibration control of large structures with information constraints

F. Palacios-Quiñonero[a,*], J. Rubió-Massegú[a], J. M. Rossell[a], H. R. Karimi[b]

[a]*Dept. of Mathematics, Universitat Politècnica de Catalunya (UPC), Av. Bases de Manresa, 61-73, 08242-Manresa, Spain*
[b]*Politecnico di Milano, Department of Mechanical Engineering, via La Masa 1, 20156 Milan, Italy*

Abstract

In this paper, we present an effective computational strategy to design high-performance decentralized controllers with partial local-state information for vibration control of large building structures. In the proposed approach, the overall building model is first decomposed into a set of approximate low-dimensional decoupled subsystems subject to the action of generalized disturbances, which include the effect of external physical disturbances, modeling approximation errors and mechanical subsystem interactions. Next, using the approximate decoupled subsystems, an overall structured state-feedback controller is obtained by designing a proper set of independent local controllers. The proposed computational strategy is applied to obtain two structured control systems for the seismic protection of a 35-story building: (i) a fully decentralized velocity-feedback controller with 35 interstory actuators that can be passively implemented by a set of viscous dampers, and (ii) a decentralized velocity-feedback controller with 15 interstory actuators, which can be implemented with a reduced set of collocated sensors and a system of five independent short-range communication networks. To assess the performance of the obtained structured controllers, the corresponding frequency and time responses are investigated and compared with the responses produced by optimal full-state H_∞ controllers. Moreover, to evaluate the effectiveness of the computational procedure, structured and full-state controllers are designed for a proper set of buildings with different number of stories and the corresponding computation times are recorded and compared. The obtained results show that the computational cost of the proposed design methodology is remarkably low and also indicate that, despite the severe information constraints, the synthesized structured controllers are practically optimal.

Keywords: structural vibration control, decentralized control, linear matrix inequalities, seismic control

1. Introduction

For vibration control of large structures, the idea of using a distributed control system formed by a large number of smart control devices that work jointly to mitigate the overall vibration response is certainly an appealing concept [1–5]. Considering the current technological means, designing smart control devices that integrate actuation mechanisms, sensors, communication units and computational capabilities is a clearly solvable issue [6, 7]. In contrast, designing suitable controllers to drive a large number of such devices is still a challenging and complex open problem, which

*Corresponding author
Email addresses: francisco.palacios@upc.edu (F. Palacios-Quiñonero), josep.rubio@upc.edu (J. Rubió-Massegú), josep.maria.rossell@upc.edu (J. M. Rossell), hamidreza.karimi@polimi.it (H. R. Karimi)

is characterized by three fundamental elements: large dimensionality, high computational cost and severe information constraints [8–15]. For this kind of problems, design strategies based on linear matrix inequality (LMI) formulations make it possible to compute advanced controllers [16–18]. However, these strategies are only computationally effective in problems of moderate dimension. Moreover, the centralized design of decentralized controllers by setting a particular zero-nonzero pattern on the LMI variables frequently leads to infeasibility issues [19, 20].

In this paper, we present a novel controller design methodology for vibration control of large buildings equipped with a distributed system of smart control devices. The main objective is to provide an effective computational strategy to design high-performance decentralized controllers that can operate with partial local-state information. The underlying idea consists in decomposing the overall building model into a set of approximate low-dimensional decoupled subsystems subject to the action of generalized disturbances, which include the effect of physical external excitations, modeling approximation errors and mechanical subsystem interactions. Then, an overall state-feedback structured controller with partial local-state information can be efficiently computed by designing a proper set of independent local state-feedback controllers for the approximate subsystems. To demonstrate the effectiveness of the proposed design methodology, two different structured control systems with partial state information are designed for the seismic protection of a 35-story building: (i) a fully decentralized velocity-feedback controller with a complete set of 35 interstory actuators, and (ii) a partially decentralized velocity-feedback controller with an incomplete set of 15 interstory actuation devices implemented at the building bottom levels. The fully decentralized controller admits a passive implementation by means of viscous dampers. This is a simple, robust and reliable solution that can operate without sensors, no communication network and null power consumption [21, 22]. The decentralized controller requires an active or semi-active implementation and can operate with a reduced set of 15 interstory-velocity collocated sensors and a system of five independent short-range communication networks. In both cases, local sate-feedback H_∞ controllers are designed for the approximate decoupled subsystems and the performance of the overall structured controllers is evaluated by considering the frequency and time-response characteristics, taking as a reference the corresponding active full-sate H_∞ controllers. Also, to assess the computational effectiveness of the proposed methodology, the same controller designs are carried out for a set of several building models with different numbers of stories and the corresponding computation times are recorded and compared. The obtained results indicate that, despite the severe information constraints, the proposed structured controllers present a practically optimal behavior when compared with the active full-state H_∞ controllers. Moreover, the computation times required by the decentralized design procedure are remarkably small and present a well-balanced and stable increment pattern as the dimension increases. Finally, it is worth mentioning that a major effort has been made to avoid the common approach of subsystem decomposition by means of summations, and a complete matrix formulation of the computational procedure has been provided. This is certainly an important feature that facilitates a more practical and effective computational implementation.

The rest of the paper is organized as follows: In Section 2, the n-story building dynamical model for different actuation schemes is provided. In Section 3, the derivation of the decoupled subsystems is presented. In Section 4, the structured controllers with partial state information and the reference full-state H_∞ controllers are designed, and the corresponding frequency responses are compared. In Section 5, the seismic time-responses are presented and discussed.

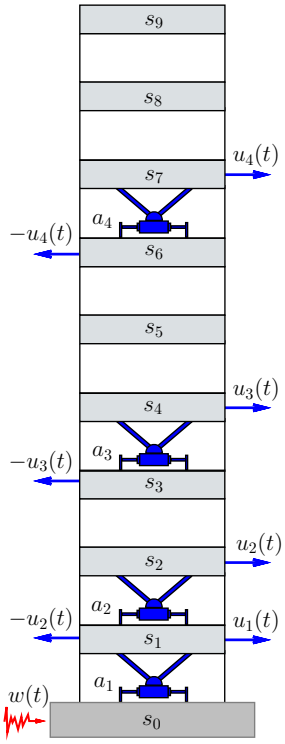

Figure 1: Multi-story building structure equipped with a system of 4 interstory force-actuation devices. Incomplete actuation scheme corresponding to the location list $L = [1, 2, 4, 7]$.

Finally, some brief conclusions are provided in Section 6.

2. Building model

Let us consider the lateral displacement of an n-story building described by the second-order model

$$\mathbf{M}\,\ddot{\mathbf{q}}(t) + \mathbf{C}_d\,\dot{\mathbf{q}}(t) + \mathbf{K}\,\mathbf{q}(t) = \mathbf{f}_u(t) + \mathbf{f}_w(t) \tag{1}$$

where $\mathbf{q}(t) = [q_1(t), \ldots, q_n(t)]^T$ is the vector of story displacements with respect to the ground, $\mathbf{M}$, $\mathbf{C}_d$ and $\mathbf{K}$ are the mass, damping and stiffness matrices, respectively, $\mathbf{f}_u(t)$ is the vector of structural control forces and $\mathbf{f}_w(t)$ is the vector of external disturbances. The mass matrix has the diagonal form $\mathbf{M} = \mathrm{diag}(m_1, \ldots, m_n)$ and the stiffness matrix has the following tridiagonal structure:

$$\mathbf{K} = \begin{bmatrix} k_1 + k_2 & -k_2 & & & & \\ -k_2 & k_2 + k_3 & -k_3 & & & \\ & \cdots & \cdots & \cdots & & \\ & & \cdots & \cdots & \cdots & \\ & & & -k_{n-1} & k_{n-1} + k_n & -k_n \\ & & & & -k_n & k_n \end{bmatrix}, \tag{2}$$

where m_i and k_i are the mass and stiffness of the ith story, respectively. If the story damping coefficients c_i are known, a tridiagonal damping matrix can be obtained by substituting the stiffness coefficients k_i in Eq. (2) by the corresponding values c_i. Frequently, however, the values c_i are unknown, and the damping matrix $\mathbf{C}_d$ is computed from $\mathbf{M}$ and $\mathbf{K}$ by setting a proper damping ratio on the building modes [23]. For seismically excited buildings, the vector of external disturbances can be written in the form $\mathbf{f}_w(t) = -\mathbf{M}\,[\mathbf{1}]_{n\times 1}\,w(t)$, where $w(t)$ is the ground acceleration input and $[\mathbf{1}]_{n\times 1}$ denotes a vector of dimension n with all its entries equal to 1. Finally, the vector of structural control forces has the form $\mathbf{f}_u(t) = \mathbf{T}_u^L\,\mathbf{u}(t)$, where $\mathbf{u}(t) = [u_1(t), \ldots, u_{n_u}(t)]^T$ is the vector of actuation forces and $\mathbf{T}_u^L$ is the control input matrix, which models the effect of the actuation forces on the structure. In this work, we assume that the n-story building is equipped with a system of $n_u \leq n$ interstory force-actuation devices implemented at different levels of the building. An actuation scheme is determined by a list of locations $L = [\ell_1, \ldots, \ell_{n_u}]$, where the location ℓ_i indicates that the actuation scheme contains an interstory actuator a_i implemented between the stories s_{ℓ_i-1} and s_{ℓ_i}, which exerts a pair of opposite structural forces of magnitude $|u_i(t)|$ upon these stories. An incomplete actuation scheme, defined by the location list $L = [1, 2, 4, 7]$, and the corresponding structural control forces are schematically depicted in Fig. 1. As it can be seen in the figure, the location $\ell_4 = 7$ indicates that the actuation scheme contains an actuator a_4, implemented between the stories s_6 and s_7, that exerts a pair of opposite structural forces of magnitude $|u_4(t)|$. For a complete actuation scheme, as the one displayed in Fig. 3(a), the location list is $[1, 2, \ldots, n]$ and the corresponding control input matrix is a square matrix of dimension n that we denote by $\mathbf{T}_u$ and has the following upper-diagonal band structure:

$$\mathbf{T}_u = \begin{bmatrix} 1 & -1 & & & & & \\ & 1 & -1 & & & & \\ & & \cdots & \cdots & & & \\ & & & \cdots & \cdots & & \\ & & & & & 1 & -1 \\ & & & & & & 1 \end{bmatrix}. \tag{3}$$

For an incomplete actuation scheme defined by the location list $L = [\ell_1, \ell_2, \ldots, \ell_{n_u}]$, $n_u < n$, the control input matrix $\mathbf{T}_u^L$ is a rectangular matrix that contains the columns of $\mathbf{T}_u$ indicated in L. Using the submatrix notations discussed in Appendix A, we can write $\mathbf{T}_u^L = \mathbf{T}_u(1, 2, \ldots, n; \ell_1, \ell_2, \ldots, \ell_{n_u})$. The interstory drift $r_i(t)$ is the relative displacement of the adjacent stories s_{i-1} and s_i, more precisely:

$$\begin{cases} r_1(t) = q_1(t) \\ r_i(t) = q_i(t) - q_{i-1}(t) \quad \text{for } \; i = 2, \ldots, n. \end{cases} \tag{4}$$

By considering the state vector

$$\mathbf{x}(t) = [r_1(t), \dot{r}_1(t), \ldots, r_n(t), \dot{r}_n(t)]^T \tag{5}$$

that presents, in increasing order, the interstory drifts and interstory velocities grouped by building levels, we obtain the state-space model:

$$\dot{\mathbf{x}}(t) = \mathbf{A}\,\mathbf{x}(t) + \mathbf{B}\,\mathbf{u}(t) + \mathbf{E}\,w(t), \tag{6}$$

with

$$\mathbf{A} = \mathbf{P}\,\widehat{\mathbf{A}}\,\mathbf{P}^{-1}, \quad \mathbf{B} = \mathbf{P}\,\widehat{\mathbf{B}}, \quad \mathbf{E} = \mathbf{P}\,\widehat{\mathbf{E}}, \tag{7}$$

$$\widehat{\mathbf{A}} = \begin{bmatrix} [\mathbf{0}]_{n\times n} & \mathbf{I}_n \\ -\mathbf{M}^{-1}\mathbf{K} & -\mathbf{M}^{-1}\mathbf{C}_d \end{bmatrix}, \quad \widehat{\mathbf{B}} = \begin{bmatrix} [\mathbf{0}]_{n\times n_u} \\ \mathbf{M}^{-1}\mathbf{T}_u^L \end{bmatrix}, \quad \widehat{\mathbf{E}} = \begin{bmatrix} [\mathbf{0}]_{n\times 1} \\ -[\mathbf{1}]_{n\times 1} \end{bmatrix}, \tag{8}$$

where $\mathbf{P}$ is the change-of-basis matrix corresponding to the state transformation

$$\mathbf{x}(t) = \mathbf{P}\begin{bmatrix} \mathbf{q}(t) \\ \dot{\mathbf{q}}(t) \end{bmatrix}, \tag{9}$$

$[\mathbf{0}]_{n\times m}$ is a zero-matrix of the indicated dimensions and $\mathbf{I}_n$ represents the identity matrix of order n. Assuming that the controller design objective is to reduce the building vibrational response by means of moderate control actions, we consider a vector of controlled outputs

$$\mathbf{z}(t) = \mathbf{C}_z\mathbf{x}(t) + \mathbf{D}_z\mathbf{u}(t) \tag{10}$$

with

$$\mathbf{C}_z = \begin{bmatrix} \mathbf{I}_{2n} \\ [\mathbf{0}]_{n_u\times 2n} \end{bmatrix}, \quad \mathbf{D}_z = \alpha\begin{bmatrix} [\mathbf{0}]_{2n\times n_u} \\ \mathbf{I}_{n_u} \end{bmatrix}, \tag{11}$$

where α is a scaling factor that compensates the different magnitude of the control forces and the state variables and can be used to adjust the intensity of the control action.

3. Decoupled substructure models

Let us consider the substructure $\mathcal{B}^{(k)}$ schematically depicted in Fig. 2, which includes n_k actuators located at the building locations $L_k = [\ell_1^k, \ldots, \ell_{n_k}^k]$, and a set of collocated sensors that provide the information corresponding to m_k components of the state vector specified by the list of positions $J_k = [j_1^k, \ldots, j_{m_k}^k]$. The first objective is to formulate an approximate local model

$$\dot{\mathbf{x}}^{(k)}(t) = \mathbf{A}^{(k)}\,\mathbf{x}^{(k)}(t) + \mathbf{B}^{(k)}\,\mathbf{u}^{(k)}(t) + \mathbf{E}^{(k)}\,\mathbf{w}^{(k)}(t), \tag{12}$$

where the state vector $\mathbf{x}^{(k)}(t)$ includes the locally measurable state information, and the control vector $\mathbf{u}^{(k)}(t)$ contains the control actions corresponding to the actuation devices implemented in the substructure. The local disturbance vector $\mathbf{w}^{(k)}(t)$ is a generalized disturbance that includes the effect of external physical excitations, local modeling errors and mechanical interactions with neighboring substructures. We also want to define a suitable local controlled-output vector

$$\mathbf{z}^{(k)}(t) = \mathbf{C}_z^{(k)}\mathbf{x}^{(k)}(t) + \mathbf{D}_z^{(k)}\mathbf{u}^{(k)}(t) + \mathbf{F}_z^{(k)}\,\mathbf{w}^{(k)}(t), \tag{13}$$

and design a local controller $\mathbf{u}^{(k)}(t) = \mathbf{G}^{(k)}\mathbf{x}^{(k)}(t)$, with $\mathbf{G}^{(k)} \in \mathbb{R}^{n_k\times m_k}$, that uses the partial local state information to compute the control action of the local actuators. By considering a proper set of substructures $\mathcal{B}^{(k)}$, $k = 1, \ldots, n_s$, determined by the corresponding lists of actuator locations L_k and measured state positions J_k, we can design a system of local controllers that make up an overall structured controller $\mathbf{u}(t) = \widehat{\mathbf{G}}\mathbf{x}(t)$ with a state-feedback gain matrix $\widehat{\mathbf{G}} \in \mathbb{R}^{n_u\times 2n}$ defined as follows :

$$\widehat{\mathbf{G}}_{\psi L_k}^{J_k} = \mathbf{G}^{(k)}, \quad \widehat{\mathbf{G}}_{\psi L_k}^{\overline{J}_k} = [\mathbf{0}]_{n_k\times(2n-m_k)}, \; k = 1, \ldots, n_s, \tag{14}$$

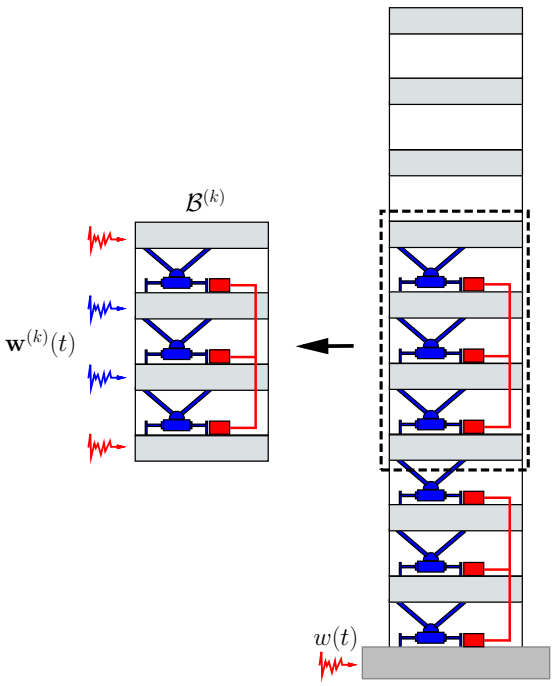

Figure 2: Decoupled substructure model and local generalized disturbance $\mathbf{w}^{(k)}(t)$, which includes the effect of external physical disturbances, local modeling errors and mechanical interactions with neighboring substructures.

where $\widehat{\mathbf{G}}_{\psi L_k}^{J_k}$ is the submatrix of $\widehat{\mathbf{G}}$ corresponding to the rows and columns specified in ψL_k and J_k, respectively, $\overline{J}_k$ denotes the complement list of J_k with respect to $[1,\ldots,2n]$, and ψL_k indicates the positions corresponding to the elements of the sublist L_k in the overall actuation list L (see Appendix A). To obtain the approximate local model in Eq. (12), we consider the global model in Eq. (6) and extract the rows corresponding to the local-state components indicated in J_k:

$$\dot{\mathbf{x}}_{J_k}(t) = [\mathbf{A}\mathbf{x}(t)]_{J_k} + [\mathbf{B}\mathbf{u}(t)]_{J_k} + [\mathbf{E}w(t)]_{J_k}\,. \tag{15}$$

By applying the decomposition property given in Eq. (A.1), we have

$$\dot{\mathbf{x}}_{J_k}(t) = \mathbf{A}_{J_k}^{J_k}\mathbf{x}_{J_k}(t) + \mathbf{A}_{J_k}^{\overline{J}_k}\mathbf{x}_{\overline{J}_k}(t) + \mathbf{B}_{J_k}^{\psi L_k}\mathbf{u}_{\psi L_k}(t) + \mathbf{B}_{J_k}^{\overline{\psi L}_k}\mathbf{u}_{\overline{\psi L}_k}(t) + \mathbf{E}_{J_k}w(t), \tag{16}$$

where $\overline{\psi L}_k$ denotes the complement of ψL_k with respect to the list $[1,\ldots,n_u]$. Next, we define the local state and control vectors

$$\mathbf{x}^{(k)}(t) = \mathbf{x}_{J_k}(t),\ \mathbf{u}^{(k)}(t) = \mathbf{u}_{\psi L_k}(t), \tag{17}$$

and the scaled local disturbance vector

$$\mathbf{w}^{(k)}(t) = \begin{bmatrix} [\mathbf{S}_x]_{\overline{J}_k}^{\overline{J}_k}\,\mathbf{x}_{\overline{J}_k}(t) \\ [\mathbf{S}_u]_{\overline{\psi L}_k}^{\overline{\psi L}_k}\,\mathbf{u}_{\overline{\psi L}_k}(t) \\ S_w\,w(t) \end{bmatrix}, \tag{18}$$

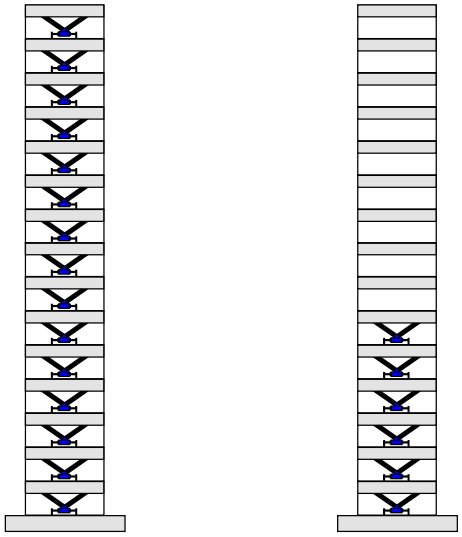

(a) Complete actuation scheme (b) Incomplete actuation scheme

Figure 3: Actuation schemes. (a) Complete actuation scheme with interstory actuation devices implemented at all building levels. (b) Incomplete actuation scheme with a reduced set of interstory actuation devices implemented at the building bottom levels.

where $\mathbf{S}_x \in \mathbb{R}^{2n\times 2n}$, $\mathbf{S}_u \in \mathbb{R}^{n_u\times n_u}$ and $S_w \in \mathbb{R}$ are scaling factors that compensate the different order of magnitude of the disturbance components. Finally, by considering the matrices

$$\mathbf{A}^{(k)} = \mathbf{A}_{J_k}^{J_k},\ \mathbf{B}^{(k)} = \mathbf{B}_{J_k}^{\psi L_k}, \tag{19}$$

$$\mathbf{E}^{(k)} = \left[\mathbf{A}_{J_k}^{\overline{J}_k}\left([\mathbf{S}_x]_{\overline{J}_k}^{\overline{J}_k}\right)^{-1} \quad \mathbf{B}_{J_k}^{\overline{\psi L}_k}\left([\mathbf{S}_u]_{\overline{\psi L}_k}^{\overline{\psi L}_k}\right)^{-1} \quad \mathbf{E}_{J_k} S_w^{-1}\right], \tag{20}$$

we obtain the approximate local model given in Eq. (12).

To define the local controlled-output in Eq.(13), we consider a new list of indexes $P_k = [p_1^k, \ldots, p_{\tilde{m}_k}^k]$, which allows selecting those components of the overall controlled-output vector $\mathbf{z}(t)$ that are relevant in the design of the local controller. From the controlled-output vector in Eq. (10), we select the rows indicted in the index list P_k and, by applying the property in Eq. (A.1), we obtain the following decomposition:

$$\mathbf{z}_{P_k}(t) = [\mathbf{C}_z]_{P_k}^{J_k}\mathbf{x}_{J_k}(t) + [\mathbf{C}_z]_{P_k}^{\overline{J}_k}\mathbf{x}_{\overline{J}_k}(t) + [\mathbf{D}_z]_{P_k}^{\psi L_k}\mathbf{u}_{\psi L_k}(t) + [\mathbf{D}_z]_{P_k}^{\overline{\psi L}_k}\mathbf{u}_{\overline{\psi L}_k}(t). \tag{21}$$

Next, by defining $\mathbf{z}^{(k)}(t) = \mathbf{z}_{P_k}(t)$ and considering the local state and control vectors in Eq. (17), and the local scaled disturbance in Eq. (18), we obtain the following local controlled-output matrices:

$$\mathbf{C}_z^{(k)} = [\mathbf{C}_z]_{P_k}^{J_k},\ \mathbf{D}_z^{(k)} = [\mathbf{D}_z]_{P_k}^{\psi L_k}, \tag{22}$$

$$\mathbf{F}_z^{(k)} = \left[[\mathbf{C}_z]_{P_k}^{\overline{J}_k}\left([\mathbf{S}_x]_{\overline{J}_k}^{\overline{J}_k}\right)^{-1} \quad [\mathbf{D}_z]_{P_k}^{\overline{\psi L}_k}\left([\mathbf{S}_u]_{\overline{\psi L}_k}^{\overline{\psi L}_k}\right)^{-1} \quad [\mathbf{0}]_{\tilde{m}_k\times 1}\right]. \tag{23}$$

For the building model presented in Section 2, the different elements of the proposed general decomposition procedure have the following particular characteristics:

Actuator locations. The actuation devices are located at the building positions indicated in the list $L = [\ell_1, \ldots, \ell_{n_u}]$.

The subsystems actuation lists L_k, $k = 1, \ldots, n_s$, are a partition of L, that is, they cover the whole list L and have no common elements.

Measured states. In the proposed building model, we assume that the actuation devices have an associated sensing unit that allows measuring the corresponding interstory drift and/or interstory velocity. In Fig. 2, these collocated sensors are schematically represented by small red boxes attached to associated interstory actuators. Considering the structure of the state vector in Eq. (5), the sensing unit associated to the actuation device a_i, and implemented in the building position ℓ_i, can provide the state components $x_{2\ell_i-1}(t) = r_{\ell_i}(t)$ and/or $x_{2\ell_i}(t) = \dot{r}_{\ell_i}(t)$. Hence, the list $J_k^d = 2L_k - 1$ provides the positions of the local interstory drifts in the global state vector. Analogously, the global-state position list of the local interstory velocities is $J_k^v = 2L_k$. We can indicate that the local feedback information includes all the locally available interstory drifts and velocities by choosing the list of state components $J_k = J_k^d \cup J_k^v$. For a local velocity-feedback controller, the list of measured-state components is $J_k = J_k^v$.

Controlled-output components. To define the local controlled-output vector $\mathbf{z}^{(k)}(t)$, we select the components of the global controlled-output vector $\mathbf{z}(t)$ indicated in the list of positions P_k. In this case, a natural choice consists in including the controlled-output components corresponding to the local state and the local control actions. According to Eq. (10), the global controlled-output vector has the following structure:

$$\mathbf{z}(t) = [r_1(t), \dot{r}_1(t), \ldots, r_n(t), \dot{r}_n(t), \alpha u_1(t), \ldots, \alpha u_{n_u}(t)]^T. \tag{24}$$

Hence, we can select the list of controlled-outputs:

$$P_k = [2L_k - 1] \cup [2L_k] \cup [\psi L_k + 2n]. \tag{25}$$

Scaling factors. The definition of the scaled local disturbance $\mathbf{w}^{(k)}(t)$ in Eq. (18) involves three scaling factors $\mathbf{S}_x \in \mathbb{R}^{2n\times 2n}$, $\mathbf{S}_u \in \mathbb{R}^{n_u\times n_u}$, and $S_w \in \mathbb{R}$, which can be taken with the following form:

$$\mathbf{S}_x = \text{diag}(\beta_d, \beta_v, \ldots, \beta_d, \beta_v), \quad \mathbf{S}_u = \beta_u \mathbf{I}_m, \quad S_w = \beta_w. \tag{26}$$

Interstory drifts in the order of 10^{-2}m, interstory velocities in the order of 10^{-1}m/s, control forces in the order of 10^6N and ground accelerations in the order of 10^0m/s^2 are common in structural vibration control problems of large buildings. Accordingly, the following values of the scaling coefficients can be selected:

$$\beta_d = 100,\ \beta_v = 10,\ \beta_u = 10^{-6},\ \beta_w = 1. \tag{27}$$

4. Controllers designs

To illustrate the flexibility and effectiveness of the proposed computational design strategy, we consider a 35-story building model equipped with two different control configurations: (i) a complete actuation scheme, with a full set of interstory actuators implemented at all building levels, and (ii) an incomplete actuation scheme, with a reduced set of interstory actuators implemented at the first 15 levels of the building. For the complete actuation scheme, a high-performance passive control system is designed by computing a fully decentralized velocity-feedback controller. For the incomplete actuation scheme, a decentralized active controller with partial state information is designed. In both cases, an ideal state-feedback H_∞ active controller with full state information is taken as the performance reference.

Table 1: Parameter values for the 35-story building model. (Taken from Lei Y, Wu DT, Lin SZ. Integration of decentralized structural control and the identification of unknown inputs for tall shear building models under unknown earthquake excitation, Eng Struct 2013;52:306–16).

story	1	2–10	11–18	19–23	24	25–27	28–33	34–35
mass ($\times 10^5$ Kg)	3.256	2.346	2.346	2.346	2.941	2.346	2.346	2.346
stiffness ($\times 10^8$N/m)	1.88	1.88	1.79	1.74	1.74	1.74	1.28	0.85
relative damping	2%							

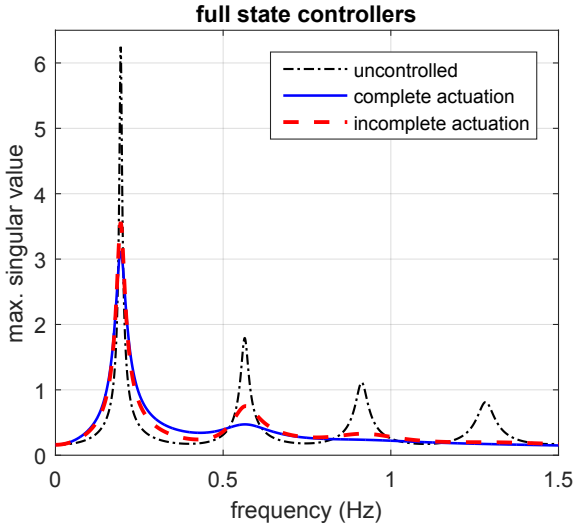

Figure 4: Frequency response corresponding to the full-state controllers defined by the control gain matrices $\mathbf{G}_1$ and $\mathbf{G}_2$. Maximum singular values of the closed-loop transfer function $T_{G_1,z_1}(\omega)$ (blue solid line), the closed-loop transfer function $T_{G_2,z_2}(\omega)$ (red dashed line) and the open-loop transfer function $T_{0,z_1}(\omega)$ (black dash-dotted line).

4.1. Passive controller with complete actuation

Let us consider the state-space model in Eq. (6) corresponding to the building parameters presented in Table 1, and the complete actuation layout schematically displayed in Fig. 3(a). In this case, the control input matrix is a square matrix of dimension $n = 35$ with the upper-diagonal band structure indicated in Eq. (3). To compute a state-feedback H_∞ controller $\mathbf{u}(t) = \mathbf{G}_1\,\mathbf{x}(t)$ for this configuration, we consider the controlled-output vector $\mathbf{z}_1(t)$ obtained in Eqs. (10) and (11) for the dimensions $n = 35$, $n_u = 35$ and the scaling factor $\alpha_1 = 10^{-6.9}$. By solving the LMI optimization problem $\mathcal{P}_0$ described in Appendix B, we obtain an optimal state-feedback gain matrix $\mathbf{G}_1 \in \mathbb{R}^{35\times 70}$ with the associated H_∞-norm $\gamma_1 = 3.1102$. The frequency response characteristics of this full-state controller are displayed in Fig. 4, where the blue solid line corresponds to the closed-loop transfer function $T_{G_1,z_1}(\omega)$ (defined in Eq. (B.7)) and the black dash-dotted line represents the frequency response of the uncontrolled building described by the open-loop transfer

Table 2: Design of the passive controller for the complete actuation scheme. Exponents of the controlled-output scaling coefficients $\alpha_{\text{pas}} = 10^{-\sigma}$ and associated H_∞-norm values with respect to the controlled-output vector $\mathbf{z}_1(t)$.

σ	6.10	6.15	6.20	6.25	6.30	6.35
γ_{pas}	3.2722	3.1792	3.1323	3.1241	3.1445	3.1830

function

$$T_{0,z_1}(\omega) = \mathbf{C}_{z_1}(2\pi\omega j\,\mathbf{I}_{2n} - \mathbf{A})^{-1}\mathbf{E}, \tag{28}$$

which can be obtained by setting a null control gain matrix in Eq. (B.7). The plots in the figure indicate that the proposed H_∞ controller is effective in reducing the building vibrational response for the main and secondaries resonant peaks. However, it should be observed that this is a centralized controller that requires the complete knowledge of the state vector to compute the control actions.

Next, for the same control setup, we design a fully decentralized controller that only uses the local interstory velocities to compute the local control actions. To build the approximate state-space local models, we select the lists of actuator locations $L_k = [k]$, $k = 1, \ldots, 35$, the lists of measured states $J_k = [2k]$, $k = 1, \ldots, 35$, and the scaling factors proposed in Eqs. (26) and (27). Additionally, to derive the local controlled-output vectors $\mathbf{z}^{(k)}(t)$, we define a global controlled-output vector $\mathbf{z}_{\text{pas}}(t)$ by setting the dimensions $n = 35$, $n_u = 35$ and a scaling coefficient α_{pas} in Eq. (11), and consider the lists of controlled-output components given in Eq. (25), which in this particular case are $P_k = [2k-1, 2k, k+70]$, $k = 1, \ldots, 35$. Finally, by applying the formulas in Eqs. (19), (20), (22) and (23), we obtain a set of $n_s = 35$ approximate local models with the following form:

$$\mathcal{S}^{(k)} : \begin{cases} \dot{\mathbf{x}}^{(k)}(t) = \mathbf{A}^{(k)}\,\mathbf{x}^{(k)}(t) + \mathbf{B}^{(k)}\,\mathbf{u}^{(k)}(t) + \mathbf{E}^{(k)}\,\mathbf{w}^{(k)}(t), \\ \mathbf{z}^{(k)}(t) = \mathbf{C}_z^{(k)}\mathbf{x}^{(k)}(t) + \mathbf{D}_z^{(k)}\mathbf{u}^{(k)}(t) + \mathbf{F}_z^{(k)}\,\mathbf{w}^{(k)}(t). \end{cases} \tag{29}$$

By solving the LMI optimization problem $\mathcal{P}$ presented in Appendix B for the local system $\mathcal{S}^{(k)}$, we obtain a local controller of the form $u_k(t) = G^{(k)}\dot{r}_k(t)$, where $G^{(k)}$ is a scalar gain, $u_k(t)$ is the control action of the k-th actuation device and $\dot{r}_k(t)$ is the associated interstory velocity. As indicated in [22], if the scalar gain $G^{(k)}$ is negative, then this local controller can be implemented by means of a viscous damper with damping constant $b_k = -G^{(k)}$. Overall, a set of negative gains $G^{(k)}$, $k = 1, \ldots, 35$, provides a particular tuning configuration for a complete system of interstory viscous dampers. The performance level of this passive control system can be evaluated by computing the corresponding H_∞-norm value γ_{pas} with respect to the controlled-output $\mathbf{z}_1(t)$ used in the design of the full-state H_∞ controller. More precisely, according to Eq. (14), the local velocity-feedback gains $G^{(k)}$ define an overall state-feedback structured controller $\mathbf{u}(t) = \mathbf{G}_{\text{pas}}\mathbf{x}(t)$ with the following control gain matrix:

$$\begin{cases} [\mathbf{G}_{\text{pas}}]_k^{2k} = G^{(k)}, & k = 1, \ldots, 35, \\ [\mathbf{G}_{\text{pas}}]_i^j = 0, & \text{otherwise.} \end{cases} \tag{30}$$

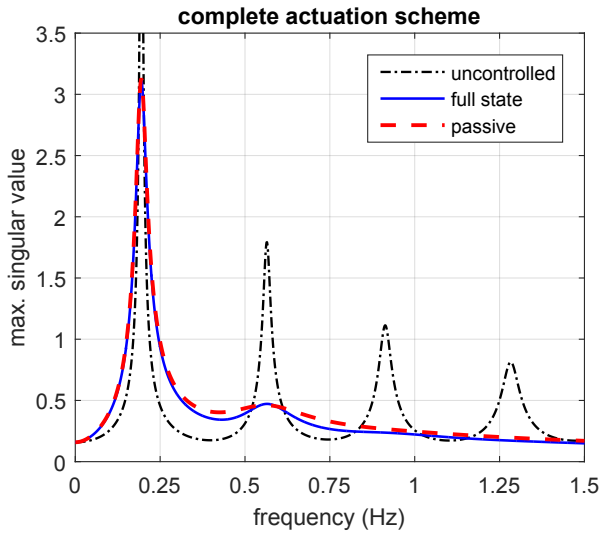

Figure 5: Frequency response corresponding to the controllers with complete actuation scheme defined by the control gain matrices $\mathbf{G}_1$ and $\mathbf{G}_{\text{pas}}$. Maximum singular values of the closed-loop transfer function $T_{G_1,z_1}(\omega)$ (blue solid line), the closed-loop transfer function $T_{G_{\text{pas}},z_1}(\omega)$ (red dashed line) and the open-loop transfer function $T_{0,z_1}(\omega)$ (black dash-dotted line).

As indicated in Appendix B, the H_∞-norm of this controller with respect to the controlled-output $\mathbf{z}_1(t)$ can be computed by solving the optimization problem

$$\gamma_{\text{pas}} = \sup_{\omega} \; \sigma_{\max}\left[T_{G_{\text{pas}},z_1}(\omega)\right], \tag{31}$$

where $T_{G_{\text{pas}},z_1}(\omega)$ is the closed-loop transfer function defined in Eq. (B.7). In order to design a high-performance passive control system, we can compare the values γ_{pas} corresponding to different scaling coefficients α_{pas}. Considering the values presented in Table 2, we have selected the scaling coefficient $\alpha_{\text{pas}} = 10^{-6.25}$, which produces a fully decentralized control system with the local velocity-feedback gains collected in Table 3 and the H_∞-norm $\gamma_{\text{pas}} = 3.1241$. This γ-value represents an increment of only 0.45% with respect to the optimal value $\gamma_1 = 3.1102$ attained by the full-state controller and it indicates that, from the H_∞ design perspective, the computed passive controller is practically optimal. A more complete view of the passive controller behavior can be obtained from the frequency response plots displayed in Fig. 5, where the red dashed line corresponds to the closed-loop transfer function $T_{G_{\text{pas}},z_1}(\omega)$, the blue solid line represents the reference closed-loop transfer function $T_{G_1,z_1}(\omega)$ and the black dash-dotted line pertains to the open-loop transfer function $T_{0,z_1}(\omega)$. Although the H_∞ controller design is only focused on minimizing the main frequency peak-value, the plots in the figure show that the proposed passive controller and the reference full-state active controller attain a similar level of performance over the complete frequency range.

4.2. Decentralized controller with incomplete actuation

In this section, we assume that the 35-story building has been equipped with an incomplete actuation system formed by $n_u = 15$ interstory actuation devices implemented at the building bottom levels, as schematically depicted in Fig. 3(b). In this case, we have the actuator location list $L = [1, 2, \ldots, 15]$, and the corresponding control input matrix $\mathbf{T}_u^L$ is a rectangular matrix of dimension 35×15 formed by the first 15 columns of the complete control input matrix

Table 3: Local velocity-feedback gains ($\times 10^7$Ns/m) for the fully decentralized controller of the complete actuation scheme.

k	$G^{(k)}$	k	$G^{(k)}$	k	$G^{(k)}$	k	$G^{(k)}$
1	−1.1734	10	−1.8676	19	−1.9451	28	−2.2902
2	−1.7752	11	−1.9133	20	−1.9439	29	−2.2693
3	−1.8922	12	−1.9175	21	−1.9437	30	−2.2650
4	−1.8797	13	−1.9162	22	−1.9441	31	−2.2618
5	−1.8755	14	−1.9159	23	−1.9461	32	−2.2556
6	−1.8735	15	−1.9157	24	−1.8376	33	−2.2253
7	−1.8734	16	−1.9155	25	−1.8368	34	−2.7750
8	−1.8717	17	−1.9151	26	−1.9432	35	−2.6137
9	−1.8708	18	−1.9114	27	−1.9235		

Table 4: Design of the decentralized controller for the incomplete actuation scheme. Exponents of the controlled-output scaling coefficients $\alpha_{\text{dec}} = 10^{-\sigma}$ and associated H_∞-norm values with respect to the controlled-output $\mathbf{z}_2(t)$.

σ	6.20	6.25	6.30	6.35	6.40	6.45
γ_{dec}	3.8374	3.7111	3.6307	3.5996	3.6119	3.6519

in Eq. (3). Using the building parameters presented in Table 1 and the matrix $\mathbf{T}_u^L$, we can compute the overall state-space model in Eq. (6) corresponding to the new actuation scheme. To design a reference state-feedback H_∞ controller $\mathbf{u}(t) = \mathbf{G}_2\,\mathbf{x}(t)$ for this new configuration, we consider the controlled-output vector $\mathbf{z}_2(t)$ obtained in Eqs. (10) and (11) with the dimensions $n = 35$ and $n_u = 15$, and the scaling factor $\alpha_2 = 10^{-6.9}$. Next, by solving the corresponding LMI optimization problem $\mathcal{P}_0$, we obtain an optimal state-feedback gain matrix $\mathbf{G}_2 \in \mathbb{R}^{15\times 70}$ with the associated H_∞-norm $\gamma_2 = 3.5545$. The frequency response characteristics of this full-state controller are displayed in Fig. 4, where the red dashed line corresponds to the closed-loop transfer function $T_{G_2,z_2}(\omega)$ and the black dash-dotted line represents the frequency response of the uncontrolled building. The plots in the figure indicate that this second state-feedback controller provides a significant level of reduction in the building vibrational response. It can also be appreciated a moderate loss of performance with respect to the optimal state-feedback controller with complete actuation scheme (blue solid line), which can be explained by the reduced number of actuation devices.

From a practical perspective, the controller defined by the state-gain matrix $\mathbf{G}_2$ presents the serious drawback of requiring the complete building state information to compute the corresponding control actions. To illustrate the effectiveness and flexibility of the proposed design strategy, we next decompose the actuated part of the building into a system of five decoupled three-story substructures $\mathcal{B}^{(k)}$ (as the one schematically displayed in Fig. 2) and design a set of local velocity-feedback controllers that can compute the actions of the local actuators from the interstory velocities

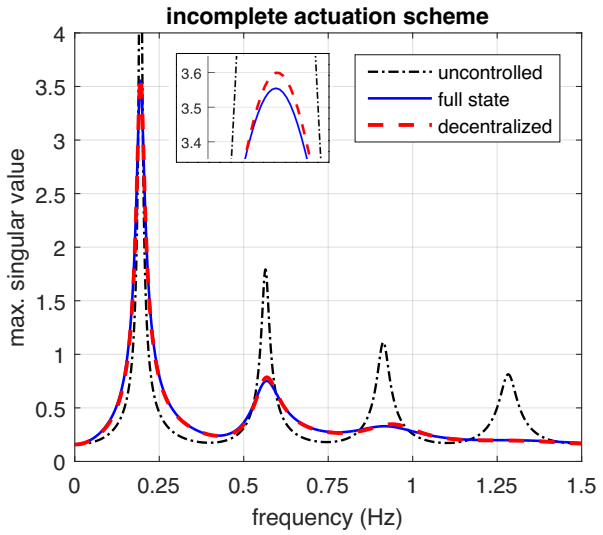

Figure 6: Frequency response corresponding to the controllers with incomplete actuation scheme defined by the control gain matrices $\mathbf{G}_2$ and $\mathbf{G}_{\text{dec}}$. Maximum singular values of the closed-loop transfer function $T_{G_2,z_2}(\omega)$ (blue solid line), the closed-loop transfer function $T_{G_{\text{dec}},z_2}(\omega)$ (red dashed line) and the open-loop transfer function $T_{0,z_2}(\omega)$ (black dash-dotted line).

provided by the associated local sensors. To build the approximate state-space local models, we select the lists of actuator locations $L_k = [3k-2, 3k-1, 3k]$, $k = 1,\ldots,5$, the lists of measured states $J_k = 2L_k$, $k = 1,\ldots,5$, and the scaling matrices proposed in Eqs. (26) and (27). We also define a global controlled-output vector $\mathbf{z}_{\text{dec}}(t)$ by setting the dimensions $n = 35$, $n_u = 15$ and a scaling coefficient α_{dec} in Eq. (11), and consider the lists of controlled-output components $P_k = [2L_k - 1] \cup [2L_k] \cup [\psi L_k + 70]$, $k = 1,\ldots,5$, to derive the local controlled-output vectors $\mathbf{z}^{(k)}(t)$. Finally, by applying the formulas in Eqs. (19), (20), (22) and (23), we obtain a system of decoupled approximate local models $\mathcal{S}^{(k)}$, $k = 1,\ldots,5$, with the form given in Eq. (29).

By solving the LMI optimization problem $\mathcal{P}$ corresponding to the local system $\mathcal{S}^{(k)}$, we can obtain a local controller of the form $\mathbf{u}^{(k)}(t) = \mathbf{G}^{(k)}\mathbf{x}^{(k)}(t)$, where $\mathbf{G}^{(k)}$ is a gain matrix of dimensions 3×3, $\mathbf{u}^{(k)}(t)$ is a vector of dimension 3 with the control actions corresponding to the actuators in the building positions L_k, and $\mathbf{x}^{(k)}(t)$ is a vector that contains the interstory velocities corresponding to the building levels L_k. As it happened in the previous section, the control gain matrices $\mathbf{G}^{(k)}$, $k = 1,\ldots,5$, define a global state-feedback structured controller $\mathbf{u}(t) = \mathbf{G}_{\text{dec}}\mathbf{x}(t)$, and the design procedure can be adjusted by setting a proper value of the parameter α_{dec}, which can be obtained by considering the H_∞-norm of the overall structured controller with respect to the controlled-output vector $\mathbf{z}_2(t)$:

$$\gamma_{\text{dec}} = \sup_{\omega} \ \sigma_{\max}\left[T_{G_{\text{dec}},z_2}(\omega)\right]. \tag{32}$$

Looking at the values presented in Table 4, we select the scaling coefficient $\alpha_{\text{dec}} = 10^{-6.35}$ and design the following set of local control matrices:

$$\mathbf{G}^{(1)} = 10^6 \times \begin{bmatrix} -6.3015 & -2.0113 & -1.2502 \\ -2.9154 & -6.1421 & -1.4619 \\ -3.7483 & -3.0797 & -5.8210 \end{bmatrix}, \tag{33}$$

$$\mathbf{G}^{(2)} = 10^6 \times \begin{bmatrix} -8.8139 & -5.6369 & -4.1763 \\ -3.8322 & -9.3853 & -3.8275 \\ -4.1665 & -5.6173 & -8.7939 \end{bmatrix}, \tag{34}$$

$$\mathbf{G}^{(3)} = 10^6 \times \begin{bmatrix} -8.7435 & -5.5453 & -4.1102 \\ -3.7673 & -9.3189 & -3.7658 \\ -4.1079 & -5.5400 & -8.7385 \end{bmatrix}, \tag{35}$$

$$\mathbf{G}^{(4)} = 10^6 \times \begin{bmatrix} -9.2187 & -6.0036 & -4.3778 \\ -3.8557 & -9.2980 & -3.7554 \\ -4.0797 & -5.4092 & -8.5267 \end{bmatrix}, \tag{36}$$

$$\mathbf{G}^{(5)} = 10^6 \times \begin{bmatrix} -9.4322 & -6.1221 & -4.4215 \\ -3.9465 & -9.4943 & -3.7301 \\ -3.9326 & -5.1522 & -8.4039 \end{bmatrix}. \tag{37}$$

The frequency response of the global structured controller defined by the local control matrices $\mathbf{G}^{(k)}$, $k = 1, \ldots, 5$, is displayed in Fig. 6, where the red dashed line corresponds to the closed-loop transfer function $T_{G_{\text{dec}}, z_2}(\omega)$, the blue solid line represents the reference closed-loop transfer function $T_{G_2, z_2}(\omega)$ and the black dash-dotted line presents the uncontrolled response. In the zoomed region, it can be appreciated a small difference (of about 1.3%) in the main peak-values $\gamma_{\text{dec}} = 3.5996$ and $\gamma_2 = 3.5545$ attained by the proposed structured controller and the reference full-state feedback controller, respectively. For all the other frequencies, the response of both control configurations are practically equal.

Remark 1. The value $\alpha = 10^{-6.9}$ used in the computation of the full-state control gain matrices $\mathbf{G}_1$ and $\mathbf{G}_2$ has been selected based on the frequency-response plots in Fig. 4 and the time-response peak-values presented in Section 5. To provide a meaningful performance evaluation, the structured controllers defined by the overall gain matrices $\mathbf{G}_{\text{pas}}$ and $\mathbf{G}_{\text{dec}}$ have been designed taking the full-state γ-values as a reference. However, from a practical point of view, it should be observed that computing a reference full-state controller is not a necessary step in the design of the proposed structured controllers, which can be independently computed based on their own frequency and time responses.

Remark 2. To obtain a meaningful comparison of two closed-loop frequency responses, the same controlled-output vector must be used in the corresponding transfer functions. For the plots in Fig. 4, however, it should be noted that the open-loop transfer functions $T_{0, z_1}(\omega)$ and $T_{0, z_2}(\omega)$ only differ in a number of null rows and, consequently, they have the same positive singular values for all the frequencies. Considering this fact, the frequency response of the reference full-state controllers can be indirectly compared by using the transfer functions $T_{G_1, z_1}(\omega)$, $T_{G_2, z_2}(\omega)$ and the common open-loop frequency response.

Remark 3. For the actuation schemes considered in this section, the actuator building locations and their corresponding positions in the overall actuation list $L = [\ell_1, \ldots, \ell_{n_u}]$ are coincident. That its, for an actuator device implemented at the k-th building level, we have the value $\ell_k = k$ in the actuation list. Hence, in this case, the local actuation lists

Table 5: Total computation time (in seconds) corresponding to the design of full-state controllers and passive controllers for an n-story building with a complete actuation scheme.

n	15	20	25	30	35
full state	29.58	609.83	1018.92	2578.95	6711.24
passive	1.03	3.44	7.04	16.71	27.32

Table 6: Total computation time (in seconds) corresponding to the design of full-state controllers and decentralized controllers for an n-story building with an actuation scheme of 15 actuators implemented at the building bottom levels.

n	15	20	25	30	35
full state	16.41	111.18	1719.77	1200.29	11227.67
decentralized	0.64	0.97	1.61	2.21	2.79

satisfy $\psi L_k = L_k$. However, it should be observed that, in general, the actuator building location and its position in the overall actuation list L can take different values and, consequently, the case $\psi L_k \neq L_k$ must be considered in the general formulation.

4.3. Computational cost

To evaluate the computational effectiveness of the proposed design methodology, we have recorded the computation times corresponding to the design of full-state and structured controllers for a proper set of n-story buildings. More precisely, for $n = 15$, 20, 25, 30 and 35, we have considered the building models corresponding to the first n stories of the 35-story building used in the previous sections. For these n-story building models, we have computed full-state and passive controllers with a complete actuation scheme, as those designed in Section 4.1, obtaining the computation times collected in Table 5. Next, we have assumed that the n-story buildings are equipped with a system of 15 interstory actuators implemented at the building bottom levels and, for this actuation scheme, we have designed full-state controllers and decentralized controllers with the same structure considered in Section 4.2. The computation times corresponding to this second control configuration are presented in Table 6. The obtained data clearly show the uncontrolled growth of the computational time corresponding to the full-state designs. Also, the data in Table 6 seem to indicate that the LMI solver has encountered additional difficulties in the case of the full-state controllers with incomplete actuation scheme. In contrast, the computational times observed in the passive and decentralized controller designs are remarkably low and maintain a stable and well-balanced growth pattern. To gain a clearer insight into the computational effectiveness of the proposed approximate design strategy, it can be observed that obtaining the full-state gain matrix $\mathbf{G}_2$ has required a computation time of about 3.12 hours, while the set of six structured controllers computed in Table 4 to obtain a suitable α-value for the decentralized controller design has required an overall computation time inferior to 18 seconds.

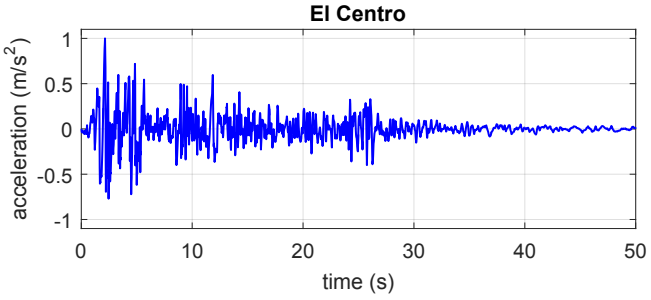

Figure 7: North-South component of the El Centro 1940 seismic record scaled to an acceleration peak of 1m/s^2.

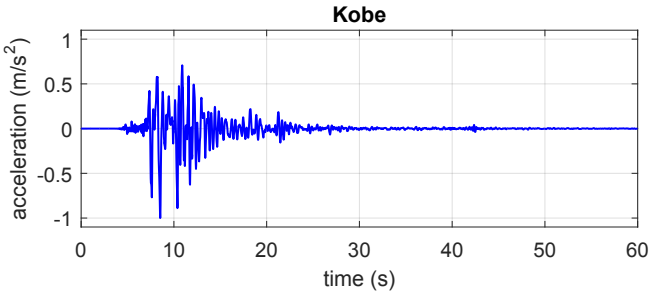

Figure 8: North-South component of the Kobe 1995 seismic record scaled to an acceleration peak of 1m/s^2.

Remark 4. All the computations in this paper have been performed using Matlab© R2016b on a regular laptop with an Intel© Core™ i7-5500U processor at 2.40 GHz. The LMI optimization problems corresponding to the different controller designs have been solved with the function `mincx()` included in the Robust Control Toolbox™, and a relative accuracy of 10^{-5} has been set in the LMI solver options.

5. Seismic response

To demonstrate the behavior of the proposed structured controllers, in this section we carry out a set of numerical simulations of the 35-story building seismic response using two different seismic records as ground acceleration input: the North-South El Centro 1940 (see Fig. 7) and the North-South Kobe 1995 (see Fig. 8). To facilitate a meaningful comparison of the results, both seismic records have been scaled to an acceleration peak-value of 1m/s^2. The peak-values of the interstory drifts, story absolute accelerations and control efforts corresponding to the complete actuation scheme and the El Centro seismic disturbance are displayed in Fig. 9. In this figure, the red dashed lines with asterisks present the seismic response of the structured control system defined by the overall control matrix $\mathbf{G}_{\text{pas}}$, the blue solid lines with circles show the response of the reference full-state controller defined by the control gain matrix $\mathbf{G}_1$, and the black solid lines with squares present the uncontrolled building response. The plots in Fig. 9(a) and Fig. 9(b) show that both controllers achieve a good and similar level of reduction in the interstory drift and absolute acceleration peak-values with respect of the uncontrolled response. The plots in Fig. 9(c) also indicate that slightly larger control-effort peak-values are produced by the passive controller. However, it should be noted that this controller can be implemented by means of viscous passive dampers and, consequently, the control forces can be generated in this case with

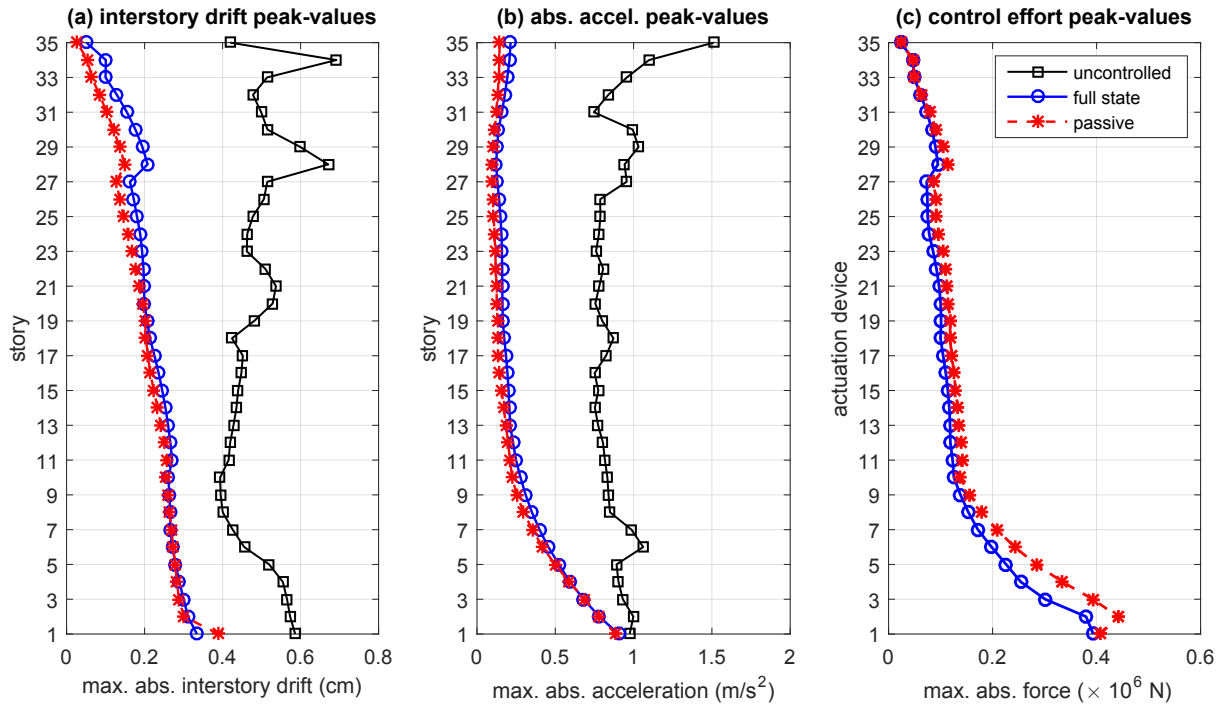

Figure 9: Seismic response of the 35-story building with complete actuation scheme corresponding to the uncontrolled configuration (black line with rectangles), the full-state controller $\mathbf{u}(t) = \mathbf{G}_1\,\mathbf{x}(t)$ (blue line with circles), and the passive controller $\mathbf{u}(t) = \mathbf{G}_{\text{pas}}\mathbf{x}(t)$ (red dashed line with asterisks). (a) Interstory drift peak-values. (b) Story absolute-acceleration peak-values. (c) Control effort peak-values. The scaled North-South El Centro 1940 seismic record has been used as ground acceleration disturbance.

null power consumption. For both controllers, the interstory-velocity and control-force time histories corresponding to the building 15th level are displayed in Fig. 10, where it can be clearly appreciated the passive character of the control actions generated by the structured controller. The seismic response of the 35-story building with incomplete actuation scheme is presented in Fig. 11. In this case, the scaled Kobe 1995 seismic record has been used as input disturbance, the red dashed lines with asterisks show the response of the structured control system defined by the overall control matrix $\mathbf{G}_{\text{dec}}$, the blue solid lines with circles display the response of the reference full-state controller with control gain matrix $\mathbf{G}_2$, and the black solid lines with squares represent the uncontrolled building response. Looking at the plots in Fig. 11(a) and Fig. 11(b), it can be appreciated that both controllers attain an appreciable reduction of the building response and that slightly larger interstory-drift and absolute-acceleration peak-values are produced by the structured controller, which is consistent with the reduced control effort peak-values observed in Fig. 11(c). It should be noted that, in this case, the practical implementation of both controllers will demand the usage of active actuation devices. However, the required sensing and communication systems are very different. The full-state controller requires a complete instrumentation of the building, with a full set of interstory-drift and interstory-velocity sensors and a wide communication system that must cover the complete building. In contrast, the proposed structured controller can operate with a reduced set of 15 interstory-velocity sensors and a system of five independent short-range communication networks (as those ones schematically represented by the red lines in Fig. 2). For this second set of controllers, the

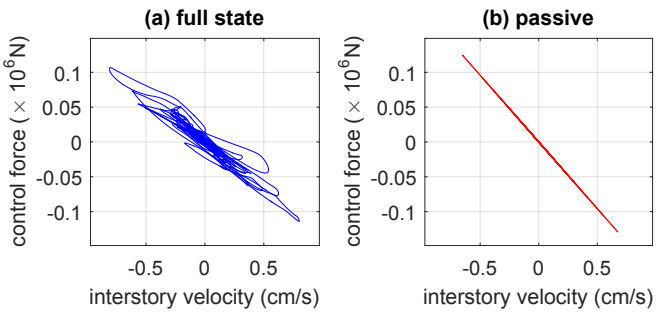

Figure 10: Complete actuation scheme. Time history of the interstory velocity and control force obtained in the building 15th level for the scaled El Centro 1940 seismic disturbance. (a) Full-state controller with control gain matrix $\mathbf{G}_1$. (b) Passive controller with overall control gain matrix $\mathbf{G}_{\text{pas}}$.

interstory-velocity and control-force time history records corresponding to the building 15th level can be observed in Fig. 12.

6. Conclusions and future directions

In this paper, a novel computational design strategy for vibration control of large buildings has been presented. Following the proposed methodology, the overall building model can be decomposed into a set of approximate low-dimensional decoupled subsystems subject to generalized disturbances, and high performance structured controllers with partial local-state information can be designed with a remarkably low computational cost. The obtained results indicate that the proposed computational strategy can be an effective tool to cope with some relevant issues commonly encountered in vibration control designs for large-scale structures, such as parameter uncertainties, hard time-constraints, sensor and actuator failures, and random communication delays. Certainly, there exists a wide variety of solutions to this kind of issues but, in most cases, the direct application of these design methodologies to large-dimension problems is totally ineffective due to the huge increase in the computational cost.

Acknowledgments

This work was partially supported by the Spanish Ministry of Economy and Competitiveness under Grant DPI2015-64170-R/FEDER.

Appendix A. Lists and partitioned matrices

In this appendix, we present in detail some non-standard definitions and notations for lists and partitioned matrices that are extensively used in the paper. Let us consider a matrix $\mathbf{M} \in \mathbb{R}^{n_r \times n_c}$, a list of row indexes $R = [i_1, \ldots, i_{m_r}]$ and a list of column indexes $C = [j_1, \ldots, j_{m_c}]$. To avoid trivialities, we assume that the lists are non-empty, and that the indexes in a list are distinct and arranged in increasing order. The submatrix of $\mathbf{M}$ obtained by selecting the rows and columns with the indexes indicated in the lists R and C, respectively, is represented by $\mathbf{M}_R^C = \mathbf{M}(i_1, \ldots, i_{m_r}; j_1, \ldots, j_{m_c})$. If the list of row indexes is complete, that is, $R = [1, 2, \ldots, n_r]$, we use the simplified notation $\mathbf{M}^C =$

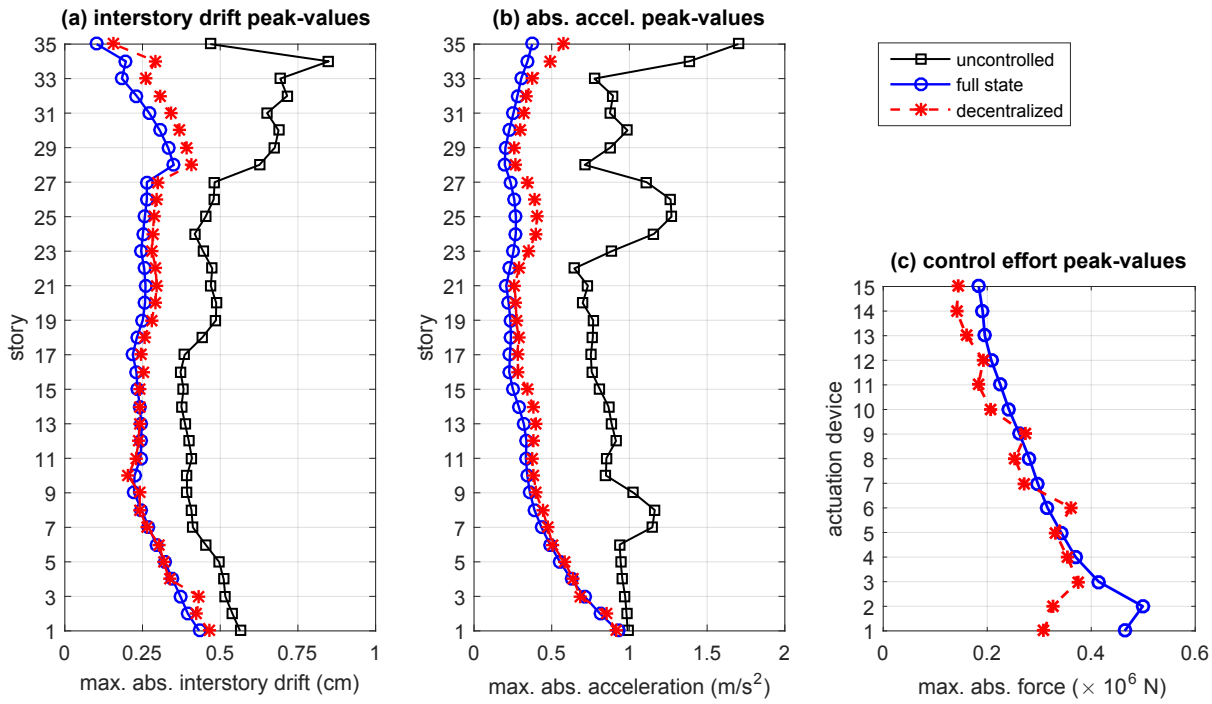

Figure 11: Seismic response of the 35-story building with incomplete actuation scheme corresponding to the uncontrolled configuration (black line with rectangles), the full-state controller $\mathbf{u}(t) = \mathbf{G}_2\,\mathbf{x}(t)$ (blue line with circles), and the decentralized controller $\mathbf{u}(t) = \mathbf{G}_{\text{dec}}\mathbf{x}(t)$ (red dashed line with asterisks). (a) Interstory drift peak-values. (b) Story absolute-acceleration peak-values. (c) Control effort peak-values. The scaled North-South Kobe 1995 seismic record has been used as ground acceleration disturbance.

$\mathbf{M}(1,\ldots,n_r\,;j_1,\ldots,j_{m_c})$. Analogously, the simplified notation $\mathbf{M}_R = \mathbf{M}(i_1,\ldots,i_{m_r};1,\ldots,n_c)$ is used when the list of column indexes is complete. For a vector $\mathbf{v} = [v_1,\ldots,v_{n_v}]^T$ and a list of element indexes $E = [i_1,\ldots,i_{m_e}]$, we set $\mathbf{v}_E = [v_{i_1},\ldots,v_{i_{m_e}}]^T$. Given a matrix $\mathbf{M} \in \mathbb{R}^{n_r\times n_c}$, a list of rows R, a list of columns C and a vector $\mathbf{v} \in \mathbb{R}^{n_c}$, the following useful decomposition of the product $\mathbf{Mv}$ can be performed:

$$[\mathbf{Mv}]_R = \mathbf{M}_R\,\mathbf{v} = \mathbf{M}_R^C\,\mathbf{v}_C + \mathbf{M}_R^{\overline{C}}\,\mathbf{v}_{\overline{C}}\,, \tag{A.1}$$

where $\overline{C}$ denotes the complement of C with respect to the complete list of column indexes $[1,\ldots,n_c]$. For a given list of indexes $L = [\ell_1,\ldots,\ell_n]$, a sublist $S = [s_1,\ldots,s_m]$ can be obtained by selecting m elements from L. In this case, we use the notation $\psi(s_i)$ to indicate the position of the sublist element s_i in the main list L. We also use the notation $\psi S = [\psi(s_1),\ldots,\psi(s_m)]$ for the complete list of positions corresponding to all the sublist elements s_i in the list L. Thus, for example, from the main list $L = [3,5,6,8,10]$, we can extract the sublist $S = [3,8,10]$. The sublist element $s_2 = 8$ has the position $\psi(s_2) = 4$ in the main list L and, for the complete sublist, we have $\psi S = [1,4,5]$. The complement of S with respect to L is $\overline{S} = [5,6]$. Finally, for $a,b \in \mathbb{N}$ and $L = [\ell_1,\ldots,\ell_n]$, we set $aL + b = [a\cdot\ell_1 + b,\ldots,a\cdot\ell_n + b]$.

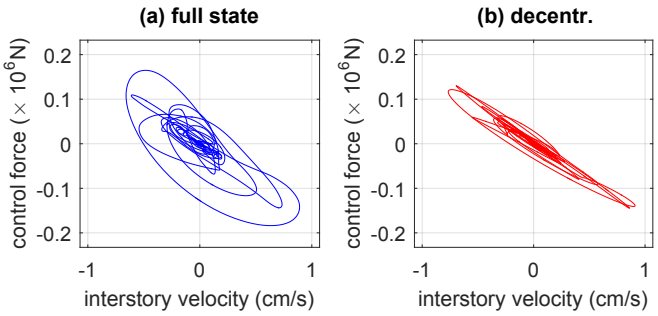

Figure 12: Incomplete actuation scheme. Time history record of the interstory velocity and control force obtained in the building 15th level for the scaled Kobe 1995 seismic disturbance. (a) Full-state controller with control gain matrix $\mathbf{G}_2$. (b) Decentralized controller with overall control gain matrix $\mathbf{G}_{\text{dec}}$.

Appendix B. H_∞ controller design

This appendix provides a brief summary of the state-feedback H_∞ controller design methodology. Let us consider a linear system in the form:

$$\begin{cases} \dot{\mathbf{x}}(t) = \mathbf{A}\,\mathbf{x}(t) + \mathbf{B}\,\mathbf{u}(t) + \mathbf{E}\,\mathbf{w}(t), \\ \mathbf{z}(t) = \mathbf{C}_z\,\mathbf{x}(t) + \mathbf{D}_z\,\mathbf{u}(t) + \mathbf{F}_z\mathbf{w}(t), \end{cases} \tag{B.1}$$

where $\mathbf{x}(t)$ is the state, $\mathbf{u}(t)$ is the control action, $\mathbf{w}(t)$ is the external disturbance, $\mathbf{z}(t)$ is the controlled output, and $\mathbf{A}$, $\mathbf{B}$, $\mathbf{E}$, $\mathbf{C}_z$, $\mathbf{D}_z$ and $\mathbf{F}_z$ are constant matrices of appropriate dimensions. A state-feedback controller $\mathbf{u}(t) = \mathbf{G}\mathbf{x}(t)$ defines the closed-loop system

$$\begin{cases} \dot{\mathbf{x}}(t) = \mathbf{A}_G\,\mathbf{x}(t) + \mathbf{E}\,\mathbf{w}(t), \\ \mathbf{z}(t) = \mathbf{C}_G\,\mathbf{x}(t) + \mathbf{F}_z\mathbf{w}(t), \end{cases} \tag{B.2}$$

with $\mathbf{A}_G = \mathbf{A} + \mathbf{B}\mathbf{G}$ and $\mathbf{C}_G = \mathbf{C}_z + \mathbf{D}_z\mathbf{G}$. The design objective is to obtain an optimal controller $\mathbf{u}(t) = \widetilde{\mathbf{G}}\mathbf{x}(t)$ that produces an asymptotically stable closed-loop matrix $\mathbf{A}_{\widetilde{G}}$ and, simultaneously, minimizes the H_∞ norm of the system

$$\gamma_G = \sup_{\|\mathbf{w}\|_2 \neq 0} \frac{\|\mathbf{z}\|_2}{\|\mathbf{w}\|_2}, \tag{B.3}$$

where $\|\mathbf{f}\|_2 = \left[\int_0^\infty \mathbf{f}^T(t)\,\mathbf{f}(t)\,dt\right]^{1/2}$ is the usual continuous 2-norm. Using an LMI formulation, the optimal H_∞ controller can be obtained by solving the following convex optimization problem [16]:

$$\mathcal{P}: \begin{cases} \text{minimize } \gamma \\ \\ \text{subject to } \mathbf{X} > 0,\ \gamma > 0, \text{and the LMI in Eq. (B.4)} \end{cases}$$

$$\begin{bmatrix} \mathbf{A}\mathbf{X} + \mathbf{X}\mathbf{A}^T + \mathbf{B}\mathbf{Y} + \mathbf{Y}^T\mathbf{B}^T & * & * \\ \mathbf{E}^T & -\gamma\mathbf{I} & * \\ \mathbf{C}_z\mathbf{X} + \mathbf{D}_z\mathbf{Y} & \mathbf{F}_z & -\gamma\mathbf{I} \end{bmatrix} < 0, \tag{B.4}$$

where $*$ denotes the transpose of the symmetric entry and $\mathbf{X} = \mathbf{X}^T$, $\mathbf{Y}$ are the optimization variables. If an optimal value $\widetilde{\gamma}$ is attained in $\mathcal{P}$ for the pair $(\widetilde{\mathbf{X}}, \widetilde{\mathbf{Y}})$, then the state-feedback gain matrix $\widetilde{\mathbf{G}} = \widetilde{\mathbf{Y}}\widetilde{\mathbf{X}}^{-1}$ defines an optimal H_∞ controller

with associated γ-value $\gamma_{\widetilde{G}} = \widetilde{\gamma}$. In the particular case that $\mathbf{F}_z = \mathbf{0}$, the optimal state-feedback H_∞ controller can also be computed by solving the following simplified optimization problem:

$$\mathcal{P}_0 : \begin{cases} \text{maximize } \eta \\ \\ \text{subject to } \mathbf{X} > 0,\ \eta > 0, \text{and the LMI in Eq. (B.5)} \end{cases}$$

$$\begin{bmatrix} \mathbf{AX} + \mathbf{XA}^T + \mathbf{BY} + \mathbf{Y}^T\mathbf{B}^T + \eta\mathbf{EE}^T & * \\ \mathbf{C}_z\mathbf{X} + \mathbf{D}_z\mathbf{Y} & -\mathbf{I} \end{bmatrix} < 0. \tag{B.5}$$

In this case, if an optimal value $\widetilde{\eta}$ is attained for the pair $(\widetilde{\mathbf{X}}, \widetilde{\mathbf{Y}})$, then the state-feedback gain matrix $\widetilde{\mathbf{G}} = \widetilde{\mathbf{Y}}\widetilde{\mathbf{X}}^{-1}$ defines an optimal H_∞ controller with associated γ-value $\gamma_{\widetilde{G}} = (\widetilde{\eta})^{-1/2}$. For a given state-feedback gain matrix $\mathbf{G}$, the H_∞-norm value of the associated controller with respect to the controlled output vector $\mathbf{z}(t)$ can be computed by solving the optimization problem

$$\gamma_G = \sup_{\omega} \ \sigma_{\max}\left[T_{G,z}(\omega)\right], \tag{B.6}$$

with

$$T_{G,z}(\omega) = (\mathbf{C}_z + \mathbf{D}_z\mathbf{G})(2\pi\omega j\mathbf{I} - \mathbf{A} - \mathbf{BG})^{-1}\mathbf{E} + \mathbf{F}_z, \tag{B.7}$$

where $j = \sqrt{-1}$, ω is the frequency in hertz, and $\sigma_{\max}[\,\cdot\,]$ denotes the maximum singular value.

References

[1] Housner GW, Bergman LA, Caughey TK, Chassiakos AG, et al. Structural control: Past, present, and future. J Eng Mech–ASCE 1997;123:897–971.

[2] Spencer BF, Nagarajaiah S. State of the art of structural control. J Struct Eng–ASCE 2003;129:845–56. doi:10.1061/(ASCE)0733-9445(2003)129:7(845).

[3] Li H, Huo L. Advances in structural control in civil engineering in China. Math Probl Eng 2010;Article ID 936081:1–23. doi:10.1155/2010/936081.

[4] Korkmaz S. A review of active structural control: challenges for engineering informatics. Comput Struct 2011;89:2113–32. doi:http://dx.doi.org/10.1016/j.compstruc.2011.07.010.

[5] Basu B, Bursi OS, Casciati F, Casciati S, et al. A European Association for the Control of Structures joint perspective. Recent studies in civil structural control across europe. Struct Contr Health Monit 2014;21:1414–36. doi:10.1002/stc.1652.

[6] Spencer BF, Jo H, Mechitov KA, Li J, Sim SH, et. al. . Recent advances in wireless smart sensors for multi-scale monitoring and control of civil infrastructure. J Civil Struct Health Monit 2016;6:17–41. doi:10.1007/s13349-015-0111-1.

[7] Linderman LE, Spencer BF. Decentralized active control of multistory civil structure with wireless smart sensor nodes. J Eng Mech–ASCE 2016;142:1–10. doi:10.1061/(ASCE)EM.1943-7889.0001126.

[8] Palacios-Quiñonero F, Rodellar J, Rossell JM. Sequential design of multi-overlapping controllers for longitudinal multi-overlapping systems. Appl Math Comput 2010;217:1170–83. doi:10.1016/j.amc.2010.01.130.

[9] Lei Y, Wu DT, Lin Y. A decentralized control algorithm for large-scale building structures. Comput-Aided Civ Inf 2012;27:2–13. doi:10.1111/j.1467-8667.2010.00707.x.

[10] Lei Y, Wu DT, Lin SZ. Integration of decentralized structural control and the identification of unknown inputs for tall shear building models under unknown earthquake excitation. Eng Struct 2013;52:306–16. doi:10.1016/j.engstruct.2013.02.012.

[11] Karimi HR, Palacios-Quiñonero F, Rossell JM, Rubió-Massegú J. Sequential design of multioverlapping controllers for structural vibration control of tall buildings under seismic excitation. P I Mech Eng I-J Sys 2013;227:176–83. doi:10.1177/0959651812464026.

[12] Verdoljak RD, Linderman LE. Sparse feedback structures for control of civil systems. Struct Contr Health Monit 2016;23:1334–49. doi:10.1002/stc.1847.

[13] Cha YJ, Agrawal AK. Seismic retrofit of MRF buildings using decentralized semi-active control for multi-target performances. Earthquake Eng Struct Dyn 2017;46:409–24. doi:10.1002/eqe.2796.

[14] Bakule L, Reháb B, Papík M. Decentralized networked control of building structures. Comput-Aided Civ Inf 2016;31:871–86. doi:10.1111/mice.12225.

[15] Yan G, Chen F, Wu Y. A semi-active H_∞ control strategy with application to the vibration supression of nonlinear high-rise building under earthquake excitations. SpringerPlus 2016;5:1–17. doi:10.1186/s40064-016-2635-1.

[16] Boyd S, Ghaoui LE, Feron E, Balakrishnan V. Linear Matrix Inequalities in System and Control Theory. Philadelphia, USA: SIAM; 1994.

[17] Wang Y, Lynch JP, Law KH. Decentralized H_∞ controller design for large-scale civil structures. Earthquake Eng Struct Dyn 2009;38:377–401. doi:10.1002/eqe.862.

[18] Qu C, Huo L, Li H, Wang Y. A double homotopy approach for decentralized H_∞ control of civil structures. Struct Contr Health Monit 2014;21:269–81. doi:10.1002/stc.1552.

[19] Palacios-Quiñonero F, Rubió-Massegú J, Rossell JM, Karimi HR. Recent advances in static output-feedback controller design with applications to vibration control of large structures. Model Ident Control 2014;35:169–90. doi:10.4173/mic.2014.3.4.

[20] Palacios-Quiñonero F, Rubió-Massegú J, Rossell JM, Karimi HR. Feasibility issues in static output-feedback controller design with application to structural vibration control. J Franklin I 2014;351:139–55. doi:10.1016/j.jfranklin.2013.08.011.

[21] Yang JN, Lin S, Kim JH, Agrawal AK. Optimal design of passive energy dissipation systems based on H_∞ and H_2 performances. Earthquake Eng Struct Dyn 2002;31:921–36. doi:10.1002/eqe.130.

[22] Palacios-Quiñonero F, Rubió-Massegú J, Rossell JM, Karimi HR. Optimal passive-damping design using a decentralized velocity-feedback H_∞ approach. Model Ident Control 2012;33:87–97. doi:10.4173/mic.2012.3.1.

[23] Chopra AK. Dynamics of Structures. Theory and Applications to Earthquake Engineering. 3rd ed.; Upper Saddle River, New Jersey, USA: Prentice Hall; 2007.